THE JOURNAL OF BIOLOGICAL CHEMISTRY VOL. 282, NO. 6, pp. 3977–3988, February 9, 2007
© 2007 by The American Society for Biochemistry and Molecular Biology, Inc. Printed in the U.S.A.

Mutational Analysis of Cytochrome *b* at the Ubiquinol Oxidation Site of Yeast Complex III*

Received for publication, July 7, 2006, and in revised form, December 4, 2006 Published, JBC Papers in Press, December 4, 2006, DOI 10.1074/jbc.M606482200

Tina Wenz[‡], Raul Covian[§], Petra Hellwig[¶], Fraser MacMillan[‖], Brigitte Meunier[**], Bernard L. Trumpower[§], and Carola Hunte[‡1]

*From the [‡]Department Molecular Membrane Biology, Max Planck Institute of Biophysics, D-60438 Frankfurt am Main, Germany, the [§]Department of Biochemistry, Dartmouth Medical School, Hanover, New Hampshire 03755, the [¶]Institut de Chimie, UMR 7177 LC3, Université Louis Pasteur, 4 Rue Blaise Pascal, F-67000 Strasbourg, France, the [‖]Institute for Physical and Theoretical Chemistry and Center for Biomolecular Magnetic Resonance, Johann Wolfgang Goethe University, D-60439 Frankfurt am Main, Germany, and the **Centre de Génétique Moléculaire, CNRS, Avenue de la Terrasse, 91198 Gif-sur-Yvette, France*

The cytochrome bc_1 complex is a dimeric enzyme of the inner mitochondrial membrane that links electron transfer from ubiquinol to cytochrome *c* by a protonmotive Q cycle mechanism in which ubiquinol is oxidized at one center in the enzyme, referred to as center P, and ubiquinone is rereduced at a second center, referred to as center N. To better understand the mechanism of ubiquinol oxidation, we have examined catalytic activities and pre-steady-state reduction kinetics of yeast cytochrome bc_1 complexes with mutations in cytochrome *b* that we expected would affect oxidation of ubiquinol. We mutated two residues thought to be involved in proton conduction linked to ubiquinol oxidation, Tyr^{132} and Glu^{272}, and two residues proposed to be involved in docking ubiquinol into the center P pocket, Phe^{129} and Tyr^{279}. Substitution of Phe^{129} by lysine or arginine yielded a respiration-deficient phenotype and lipid-dependent catalytic activity. Increased bypass reactions were detectable for both variants, with F129K showing the more severe effects. Substitution with lysine leads to a disturbed coordination of a b heme as deduced from changes in the midpoint potential and the EPR signature. Removal of the aromatic side chain in position Tyr^{279} lowers the catalytic activity accompanied by a low level of bypass reactions. Pre-steady-state kinetics of the enzymes modified at Glu^{272} and Tyr^{132} confirmed the importance of their functional groups for electron transfer. Altered center N kinetics and activation of ubiquinol oxidation by binding of cytochrome *c* in the Y132F and E272D enzymes indicate long range effects of these mutations.

The mitochondrial cytochrome bc_1 complex, also termed ubiquinol:cytochrome *c* oxidoreductase (QCR)[2] or complex III, is a central component of respiratory energy conversion. The multisubunit membrane protein complex catalyzes the transfer of electrons from the membrane-localized ubiquinol to the water-soluble cytochrome *c*. This redox reaction is coupled to translocation of protons across the membrane. The mechanism that links proton translocation to electron transfer, the protonmotive Q cycle (1), depends on two spatially separated binding sites for quinol and quinone, both located in subunit cytochrome *b*. The key step of the mechanism is the bifurcated route of the two electrons released upon ubiquinol oxidation at center P. One electron is transferred into the high potential chain, the 2Fe-2S cluster Rieske protein (ISP) and cytochrome c_1, consequently being delivered to cytochrome *c*. The second electron is transferred via the low potential chain, heme b_L and heme b_H of cytochrome *b*, to center N, at which quinone is reduced to semiquinone. A complete turnover of the enzyme requires the oxidation of two ubiquinol molecules, resulting in reduction of the semiquinone (2–4).

Details of the molecular mechanism of QCR are under debate. Of special interest is the mechanism of ubiquinol oxidation at center P. The ubiquinol oxidation pocket has no direct access to the aqueous phase. A proton exit route that parallels electron transfer from ubiquinol toward heme b_L has been proposed (5, 6). Center P is mainly formed by the mitochondrial encoded cytochrome *b*. Based on crystal structures with inhibitors bound to center P and mutational studies of the bacterial QCR (5–11), several well conserved amino acid residues were suggested to play a role in ubiquinol binding, proper bifurcated electron transfer, and proton release pathways (2, 5, 6, 10). The residue Glu^{272} is proposed to be a ligand for ubiquinol and to accept protons released during ubiquinol oxidation. The residue Tyr^{132} is located between Glu^{272} and heme b_L. The hydroxyl group of this tyrosine is thought to stabilize the proton transfer pathway. The residue Tyr^{279} is proposed to preorient the substrate, whereas Phe^{129} presumably stabilizes the hydrophobic tail of the ubiquinol.

To challenge the significance of these residues for quinol catalysis, we analyzed how mutations in Glu^{272}, Tyr^{132}, Phe^{129}, and Tyr^{279} of cytochrome *b* influence ubiquinol-cytochrome *c* reductase activity and short circuit electron transfer reactions that result in superoxide anion production. We also used pre-steady-state reduction kinetics of cytochrome *b* and cytochrome c_1 of the Tyr^{132} and Glu^{272} variants to analyze the role of these residues in electron transfer.

* This work was supported by Deutsche Forschungsgemeinschaft Grant SFB 472 (to C. H., P. H., and F. M.), Boehringer Ingelheim Fonds (to T. W.), the Centre for Membrane Proteomics (to F. M.), and National Institutes of Health Grant GM 20379 (to B. L. T.). The costs of publication of this article were defrayed in part by the payment of page charges. This article must therefore be hereby marked "*advertisement*" in accordance with 18 U.S.C. Section 1734 solely to indicate this fact.

[1] To whom correspondence should be addressed: Max-Planck-Institute of Biophysics, Dept. Molecular Membrane Biology, Max-von-Laue-Str. 3, 60438 Frankfurt am Main, Germany. Tel.: 49-69-6303-1062; Fax: 49-69-6303-1002; E-mail: Carola.Hunte@mpibp-frankfurt.mpg.de.

[2] The abbreviations used are: QCR, ubiquinol:cytochrome *c* oxidoreductase; ISP, Rieske iron sulfur protein; DQH, decylubiquinol.

This is an Open Access article under the CC BY license.

EXPERIMENTAL PROCEDURES

Media and Yeast Strains—Premixed media were from For-Medium. YPGal (1% yeast extract, 2% peptone, and 3% galactose) and YPG (1% yeast extract, 2% peptone, and 3% glycerol) were used for growth of the yeast strains. The strains used in this study are described in detail elsewhere (12).

Site-directed Mutagenesis, Biolistic Transformation, and Selection of Mitochondrial Mutants—The plasmid pBM5 carrying the wild-type intronless sequence of the cytochrome *b* gene was mutagenized using the QuikChange site-directed mutagenesis kit (Stratagene). The following primers were used: 5′-CTA TTG CTA CAG CTA AAT TAG GTT ATT GTT GTG-3′ and 5′-CTC AAC AAT AAC CTA ATT TAG CAG TAG CAA TAG-3′ for F129K, 5′-CTA TTG CTA CAG CTA GAT TAG GTT ATT GTT GTG-3′ and 5′-CTC AAC AAT AAC CTA ATC TAG CTG TAG CAA TAG-3′ for F129R, and 5′-TAC AGC TTT TTT AGG TTT TTG TTG TGT TTA TG-3′ and 5′-CAT AAA CAC AAC AAA AAC CTA AAA AAG CTG TA-3′ for Y132F. The mitochondrial biolistic transformation, the selection of the mitochondrial transformants, and the integration of the mutation into the mitochondrial genome was carried out as described before (12). The yeast strains carrying the Y279A/C/S mutation were previously constructed and were provided by B. Meunier (13).

Purification of QCR—Wild-type and mutant yeast strains were grown in YPG or YPGal medium as indicated under "Results." Mitochondrial membranes were prepared as described previously (12). QCR was purified via a single DEAE Biogel column as described elsewhere applying a flow rate of 2–5 ml/min (14). Extinction coefficients of 17.5 mM^{-1} cm^{-1} for ascorbate reduced minus ferricyanide oxidized c heme (553–540 nm) and 25.6 mM^{-1} cm^{-1} for dithionite-reduced minus ferricyanide-oxidized b hemes (562–575 nm) were used for quantification of QCR.

Reconstitution of Purified QCR with Phospholipids and Determination of H^+/e^- Stoichiometry—Purified QCR was reconstituted in soy asolectin in a 1:10 molar ratio of protein to lipid. Detergent was removed by dialysis for 24 h against 100 mM KCl, 3 mM Hepes-KOH, pH 7.2. The H^+/e^- stoichiometry of the QCR reconstituted into liposomes was determined by the oxidant pulse method as previously described (12).

Measurement of Ubiquinol-Cytochrome c Reductase Activity—Ubiquinol-cytochrome *c* reductase activity of purified QCR was assayed in 50 mM KP_i, pH 7.4, 250 mM sucrose, 1 mM KCN, 0.05% *n*-undecyl-β-D-maltoside, 50 μM horse heart cytochrome *c* at room temperature. The enzyme was diluted to 2.5–10 nM in assay buffer, and the reaction was started with 40 μM decylubiquinol (DQH). Reduction of cytochrome *c* was monitored at 550 *versus* 540 nm in dual wavelength mode, and the rate of cytochrome *c* reduction was calculated with an extinction coefficient of 21.5 mM^{-1} cm^{-1}. Activity assays of reconstituted QCRs were carried out in 100 mM KCl, 3 mM Hepes-KOH, pH 7.2, 1 mM KCN, 2 μg/ml valinomycin, 40 μM DQH, and 50 μM horse heart cytochrome *c* using 2.5–10 nM QCR. Turnover numbers are expressed as mol of cytochrome *c* reduced mol^{-1} QCR s^{-1} under steady-state condition.

To determine the apparent K_m for DQH, variable concentrations of DQH (50–500 nM) were used as substrate in the activity assay with reconstituted enzyme. The concentration of the DQH stock solution was spectroscopically determined at the start of the experiment. Apparent K_m values were obtained by linear regression in an Eadie-Hofstee plot.

To determine the sensitivity to inhibitors, QCR was reconstituted with phospholipids as described above and was mixed with variable concentrations of inhibitor yielding different inhibitor/QCR ratios. The mixture was incubated for 15 min at room temperature before starting the activity assay. The concentration of the inhibitors was determined by their extinction coefficient (15). Dilutions of the inhibitors were done just before the titrations.

EPR Spectroscopy and Redox Titrations—20–40 μM purified QCR (50 mM KP_i, pH 6.9, 250 mM NaCl, 0.05% *n*-undecyl-β-D-maltoside) was reduced by the addition of excess pyrophosphate-buffered sodium dithionite at 4 °C, and the samples were immediately transferred to EPR tubes (standard suprasil quartz, outer diameter 4 mm) and frozen in liquid nitrogen. X-Band (9.4-GHz) continuous wave EPR spectra were recorded as described previously (12). Data simulation was performed using Win-Simfonia, and the measured g values were corrected for an offset against a known g standard (DPPH; with $g = 2.00351 \pm 0.00002$).

The redox titrations were performed as described before at pH 7.5 (12). Typically, data were recorded at steps of 40 mV between −0.4 and 0.2 V under anaerobic conditions. The reference electrode was calibrated with the cyclovoltammogram of a buffered $K_4(Fe(CN)_6)$ solution. All electrochemical titrations were reversible as controlled by comparing fully oxidized minus fully reduced visible spectra at different points of the experiments.

Pre-steady-state Kinetics—Pre-steady-state reduction of QCRs was followed at room temperature by stopped flow rapid scanning spectroscopy using an OLIS rapid scanning monochromator. Reactions were started by mixing 2 μM bc_1 complex in assay buffer containing either 50 mM potassium phosphate, pH 7.0, or 100 mM Tris-HCl, pH 8.8, plus 1 mM sodium azide, 1 mM EDTA, and 0.01% Tween 20 against an equal volume of the same buffer containing 40 μM DQH. A fresh solution of DQH substrate was prepared before each experiment. A spectrum of oxidized QCR was obtained by mixing the oxidized QCR against assay buffer and averaging the data sets to a single scan. For each experiment, seven or eight data sets were averaged, and the oxidized spectrum was subtracted from each scan. From the three-dimensional data set composed of wavelength, absorbance, and time, the time course and amplitude change for cytochrome *b* reduction at 563 nm or cytochrome c_1 reduction at 553 nm was extracted using the OLIS software. For the experiment in which cytochrome *c* was added, reduction of cytochrome c_1 plus cytochrome *c* was monitored at 551 nm. To obtain the maximum c_1 absorbance value, the enzyme was reduced with ascorbate. To obtain the maximum b_H absorbance, the enzyme was reduced with dithionite, and the absorbance change at 563 nm in the dithionite minus ascorbate-reduced difference spectrum was multiplied by 0.7, since the b_H heme accounts

for ~70% of the total cytochrome *b* absorbance. To calculate the expected absorbance changes at 551 nm for reduction of cytochrome *c* or reduction of cytochrome c_1 + cytochrome *c*, we used extinction coefficients of 20 mM^{-1} for cytochrome *c* and 13.7 mM^{-1} for cytochrome c_1.

RESULTS

The Ubiquinol Binding Pocket and the Location of Tyr^{132}, Phe^{129}, Glu^{272}, and Tyr^{279} at Center P—Fig. 1 shows the crystal structure of the yeast ubiquinol oxidation pocket at center P with bound competitive inhibitors and the location of the cytochrome *b* residues that were mutated for this study. The hydroxyl group of the inhibitor stigmatellin is hydrogen-bonded to the side chain of Glu^{272} (5). Hydrogen bond interaction with the Glu^{272} backbone stabilizes binding of the inhibitory substrate analogue hydroxydioxobenzothiazole (6). Glu^{272} is proposed to play an important role in ubiquinol oxidation (2, 5, 10). Recent mutagenesis studies in yeast support its relevance for accurate enzyme-substrate complex formation, prevention of electron short circuit reactions, and pH dependence of ubiquinol oxidation (12). The nearby residue Tyr^{132} is part of the binding pocket proximal to heme b_L. It stabilizes via its hydroxyl group a water molecule of the suggested proton exit relay (5). Earlier studies in bacterial QCR suggest that the equivalent Tyr^{147} is required for efficient electron transfer to heme b_L (16). The side chain of Phe^{129} is in hydrophobic interaction with the tail of stigmatellin and probably with that of the substrate. This residue is a locus of center P inhibitor resistance both in yeast and bacterial QCR (17–19). Mutational analysis of the equivalent residue in bacterial QCR (Phe^{144}) indicated that replacement of Phe^{144} affects ubiquinol binding and oxidation (9). The residue Tyr^{279} is close to the highly conserved PEWY (Pro^{271}–Tyr^{274}) motif, and it has been suggested to take part in positioning ubiquinol prior to oxidation and in stabilizing the enzyme-substrate complex by weak hydrogen bonds (6). Initial mutational studies of this residue in yeast QCR also supported a role in ubiquinol binding (13). Mutations in Tyr^{279} have been reported in patients with exercise intolerance and multisystem disorder (20), and they confer antimalarial drug resistance in *Plasmodium falciparum* QCR (21).

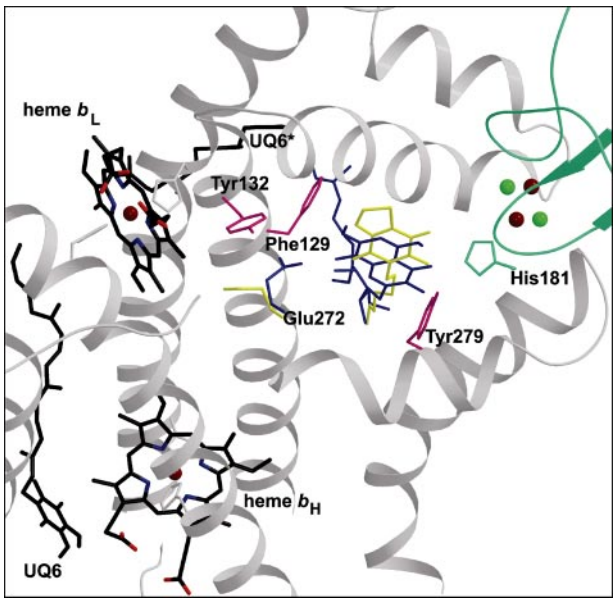

FIGURE 1. **Crystal structure of the yeast cytochrome bc_1 complex.** The section of one functional unit with cytochrome *b*, including heme cofactors and histidine ligands (*gray*) and with the [2Fe-2S] cluster Rieske protein (*green*), is viewed from the intermembrane space. The competitive inhibitors stigmatellin (*blue*, Protein Data Bank code 1EZV (5)) and hydroxydioxobenzothiazole (*yellow*, Protein Data Bank code 1P84 (6)) mark the ubiquinol binding pocket at center P. Both inhibitors are stabilized by hydrogen bonds with His^{181} of ISP and Glu^{272} of cytochrome *b*. The Glu^{272} side chain is observed in two distinct orientations dependent on center P occupancy: toward heme b_L with stigmatellin bound (*yellow*) and toward the binding pocket with hydroxydioxobenzothiazole bound (*blue*). Cytochrome *b* residues Tyr^{132}, Phe^{129}, Glu^{272}, and Tyr^{279} shown in side chain representation (*magenta*) have been targeted by mutagenesis. The natural substrate ubiquinone-6 (*UQ6*) is bound at center N. The isoprenoid tail of UQ6*, which occupies center N of the other functional unit, reaches into the hydrophobic cleft shared with center P.

Effect of Mutations on QCR Stability and Function—Growth of the mutant strains was monitored in nonfermentable medium to study a possible impact on cell respiration. The doubling time of Y132F was with 3.6 h only slightly increased compared with 3.2 h of the wild-type strain. Mutations in Tyr^{279} had a more severe effect on the respiratory growth. The Y279C strain had a doubling time of 6.4 h, and growth of Y279S (7.1 h) and Y279A (8.3 h) was even slower. Both Phe^{129} mutants did not grow on the nonfermentable media, marking F129K and F129R as lethal mutations with respect to respiration-dependent growth (Table 1). For purification of the variant QCRs, the two latter strains were grown in galactose medium, whereas all

TABLE 1

Properties of wild-type and mutant yeast strains and of the respective purified QCRs

The doubling time was measured in YPG medium for three individual cultures per strain. QCR content was determined in mitochondrial membranes by spectroscopic quantification of the b type hemes for three membrane preparations (see "Experimental Procedures"). QCR was purified via a single anion exchange chromatography. The turnover number (TN) of the purified enzymes was determined as described under "Experimental Procedures." Three preparations of enzyme per strain were carried out, and the activity measurements were repeated five times for each sample. The average error is within 10% of the given value. The K_m values were determined from an Eadie-Hofstee plot of the activity against the quotient of activity and DQH concentration. The parameter K_m for decylubiquinol (DQH) and the IC_{50} values were determined for 10 nM reconstituted QCR. Measurement of the H^+/e^- stoichiometry was carried out by the oxidant pulse method using reconstituted QCR. The respiratory control ratios of the vesicles were between 3.5 and 4.5. Each oxidant pulse experiment was carried out 6–8 times with two different enzyme preparations.

	Wild type	Y132F	Y279A	Y279C	Y279S	F129K	F129R
Doubling time on respiratory medium (h)	3.2 ± 0.2[a]	3.6 ± 0.2	8.3 ± 0.3	6.4 ± 0.4	7.1 ± 0.3	No growth	No growth
QCR content (nmol/mg protein) (% WT)	7.1 ± 0.7[a] (100%)	6.3 ± 0.2 (87%)	4.9 ± 0.6 (68%)	5.4 ± 0.4 (76%)	4.6 ± 0.7 (64%)	6.8 ± 0.7[b]	6.0 ± 0.5[b]
TN (% WT)	100[c]	48	18	55	25	27[b]	84[b]
K_m DQH (μM)	6.3[a]	53.4	3.6	9.5	3.8	33.9 [b]	3.1[b]
IC_{50} stigmatellin (nM)	2.3[a]	2.8	11.7	9.4	Resistant	Resistant[b]	8.1[b]
IC_{50} myxothiazol (nM)	2.8[a]	Resistant	13.2	6.4	Resistant	Resistant[b]	18.8[b]
H^+/e^-	2.01 ± 0.07[a]	1.96 ± 0.06	1.99 ± 0.08	1.98 ± 0.12	1.97 ± 0.07	1.45 ± 0.11[b]	2.02 ± 0.11[b]

[a] Data from Wenz *et al.* (12).
[b] Cells grown in galactose medium.
[c] TN of wild-type enzyme: 118.7 ± 9.3 s^{-1}.

other QCRs were isolated from cells grown with a mixture of glycerol and ethanol.

The effect of the mutations on QCR content was monitored by spectroscopic b heme quantification of mitochondrial membranes (Table 1). The Y132F mutant showed only a small decrease (~13%) in QCR concentration. The mutations in Tyr^{279} resulted in a more pronounced decrease. The Y279C mutant contained 76% of the wild-type level, and the Y279A (68%) and the Y279S (64%) mutants were slightly more affected. For F129K and F129R, the QCR content was determined for cells grown in galactose. In this medium, cell growth is not limited by respiration, and thus the QCR content should not be affected by the respiratory capacity of the mutant. Nevertheless, the F129R mutant had a lower QCR content than the F129K mutant, which might indicate a reduced stability of the F129R variant.

The variant enzymes were purified for further characterization. Y132F and the three variants of Y279 were purified by anion exchange chromatography without loss of activity or detectable loss of subunits as monitored with optical spectra and Western immunoblot analysis for the different purification steps (data not shown). For purification of F129R and F129K, the flow rate had to be lowered (0.6 ml/min) to prevent disintegration of the complex. We assume that the modified protein preparation retains more phospholipids, since the latter has been shown to increase complex integrity (6, 22).

The kinetic parameters of each QCR preparation were measured as described under "Experimental Procedures." The turnover numbers and K_m values for DQH are given in Table 1. Y132F QCR exhibited about half as much cytochrome *c* reductase activity as compared with the wild-type enzyme. Y279C QCR retained ~55% of the wild-type activity, whereas the alanine (18%) and serine substitutions (25%) in this position resulted in a marked decrease of the turnover number. F129K QCR exhibited an activity loss of ~75% compared with wild-type QCR, whereas F129R QCR retained 84% of the turnover. When comparing turnover numbers of the Phe^{129} variants with the wild-type enzyme, one has to note that the former may be even overestimated due to presumably higher lipid content (see above). Nevertheless, the respiratory activity of the F129R mutant is apparently not sufficient to support respiratory growth despite the substantial catalytic activity of the isolated F129R QCR and the relatively small difference in QCR content compared with F129K. The properties of F129R QCR are discussed below.

Effect of Mutations on Inhibitor Binding—The ubiquinol cytochrome *c* reductase activity of the purified QCR variants reconstituted in liposomes was measured in the presence of increasing concentrations of stigmatellin and myxothiazol to test whether the mutations change the sensitivity of the enzymes to these inhibitors. Stigmatellin binds to the niche distal to heme b_L and is proposed to mimic an intermediate of quinol oxidation (5, 6). Myxothiazol binds proximal to heme b_L (8, 15). Y132F QCR exhibits unchanged sensitivity to stigmatellin but is resistant to myxothiazol (Table 1). This agrees with results obtained for the equivalent mutation in bacterial QCR (9). Each of the substitutions in position 279 altered the sensitivity for both inhibitors. The alanine replacement caused a ~5-fold decrease in sensitivity to both inhibitors. Substitution with cysteine had a smaller effect on the sensitivity to myxothiazol, which was increased by a factor of 2.3, whereas the sensitivity to stigmatellin was increased ~4-fold. Y279S lost sensitivity to both stigmatellin and myxothiazol (Table 1). This variant did not show any decrease in cytochrome *c* reductase activity upon the addition of up to a 2000-fold excess of the inhibitors (data not shown). The different extent of inhibitor resistance in the three Tyr^{279} mutants may either reflect variable structural rearrangements in the binding pocket or different direct interactions of the substituted residues with the inhibitor. The latter is likely for stigmatellin, since the x-ray structure of the yeast complex revealed a hydrophobic interaction of Tyr^{279} and the inhibitor head group (5). A hydrophobic interaction is also present between the stigmatellin tail and Phe^{129} (5). Clearly, replacement of the aromatic side chain in position 129 by a charged residue should interfere with its binding. F129K was resistant to both stigmatellin and myxothiazol. The sensitivity of F129R to stigmatellin was decreased by 3.5-fold, and sensitivity to myxothiazol was decreased by 6.7-fold. The observed difference between lysine and arginine substitution is likewise found for substrate binding. The K_m for DQH was increased by ~6-fold for F129K, whereas it was decreased by ~2-fold for F129R, in line with the proposal that Phe^{129} stabilizes not only the hydrophobic inhibitor tail but interacts as well with the ubiquinol isoprenoid chain. Tyr^{132} is nearest to heme b_L and not in contact with stigmatellin. Accordingly, the phenylalanine substitution does not affect stigmatellin sensitivity but results in resistance to the proximal niche inhibitor myxothiazol. None of the mutations caused changes in sensitivity to the center N inhibitor antimycin (data not shown).

Superoxide Anion Production—Superoxide production is a bypass reaction of the bifurcated electron transfer at center P (24). To analyze the influence of Phe^{129}, Tyr^{132}, and Tyr^{279} mutations on this process, superoxide anion formation of the QCR variants was assayed as the superoxide dismutase-sensitive rate of cytochrome *c* reduction (Fig. 2). The difference between the reaction rate in the absence and presence of superoxide dismutase yields the contribution of cytochrome *c* reduction by superoxide anion to the overall cytochrome *c* reductase activity. As previously described, wild-type enzyme preparations are virtually free of superoxide anion production (12). In F129K, ~50% of the cytochrome *c* reduction can be attributed to superoxide. Clearly, lysine substitution markedly disturbs the bifurcated electron transfer of ubiquinol oxidation. The effect was less distinct in the F129R variant with a relative rate of superoxide anion production of ~25%. In the Y132F variant, ~20% of the cytochrome *c* reduction rate was attributed to superoxide anion. All three Tyr^{279} mutants were mildly affected and exhibited a relative superoxide anion production of 10–15%.

H^+/e^- Stoichiometry—During turnover of QCR, two protons are released at center P per one electron transferred to cytochrome *c* according to the Q cycle. Uncoupling of the Q cycle is characterized by a lowered H^+/e^- stoichiometry. To analyze the effect of the mutations on the coupling of the Q cycle, the H^+/e^- stoichiometry was determined for reconstituted enzyme by the oxidant pulse method, in which the proton

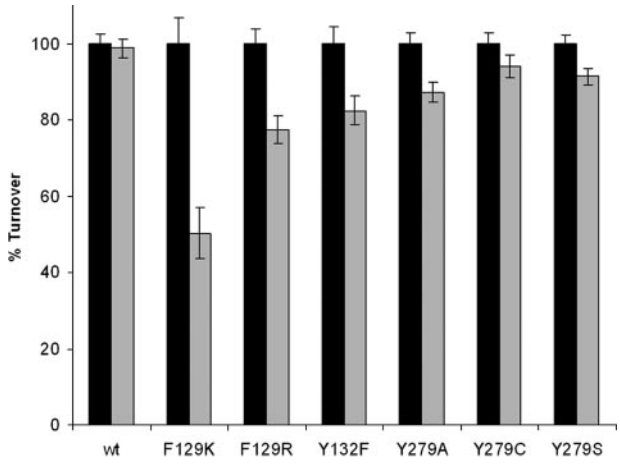

FIGURE 2. **Superoxide production in cytochrome bc_1 complex from wild-type yeast and complexes with mutations in cytochrome *b*.** The cytochrome *c* reduction rate in the absence of superoxide dismutase, shown as *black bars*, is referred to as 100% value. The respective turnover numbers of wild-type and variant QCRs are as listed in Table 1. The decreased rate with superoxide dismutase included in the assay is depicted in *gray bars*. The assay was carried out according to the standard protocol with 10 nM QCR, 50 μM cytochrome *c*, and 40 μM decyl ubiquinol supplemented with 50 units/ml catalase and 50 units/ml CuZn-superoxide dismutase. The values are the average of five measurements.

TABLE 2
Midpoint potentials of QCRs from wild-type yeast and from yeast with Y132F, F129K, and F129R mutations in cytochrome *b*

	Heme b_L	Heme b_H	Heme c_1
	mV	*mV*	*mV*
Wild type	−52	113	278
Y132F	−42	118	288
F129K	−142	8	273
F129R	−22	113	278

release at the side of center P is monitored (Table 1). As previously shown, an H^+/e^- ratio of 2 is measured for the wild-type enzyme (12). The Y132F and the three Tyr^{279} variants showed only minor deviations from that value (1.96–1.99). The F129K substitution uncoupled the Q cycle as indicated by a lowered H^+/e^- stoichiometry (1.45). In the F129R replacement, the stoichiometry was not affected. Apparently, arginine can at least partly replace phenylalanine in this position, leading to less drastic effects than for the lysine substitution. A similar effect was seen in the inhibitor binding, where F129K showed a higher resistance than F129R, and in the superoxide production assays, where the effect of the F129K mutation was markedly higher.

Redox Potentiometry—Potentiometric redox titrations were carried out to evaluate possible effects of the side chain substitutions on the midpoint potentials of the heme groups (Table 2). No major changes were observed for the Y132F mutant. In the F129K variant, both b heme potentials were shifted by approximately −100 mV. The lowered potentials of both b hemes are likely to contribute to the limitation of the F129K turnover number. In the F129R variant, the potential of heme b_L was shifted by plus 30 mV (Table 2). This is in agreement with only a slightly reduced turnover number of the isolated enzyme (Table 1). As expected, the midpoint potentials of the c_1 hemes were not affected for any of the mutations.

TABLE 3
Values for the g-tensor of the dithionite-reduced ISP in wild-type and variant QCR

Error is ±0.003 for all g values.

	Wild type[a]	F129R	Y132F	Y279A	Y279C	Y279S	E272D[a]	E272Q[a]
g_{zz}	2.025	2.025	2.025	2.021	2.021	2.020	2.017	2.024
g_{yy}	1.894	1.898	1.897	1.893	1.891	1.891	1.891	1.895
g_{xx}	1.753	1.760	1.755	1.755	1.760	1.772	1.761	1.749

[a] From Ref. 12.

EPR Analysis of Center P—EPR spectra were recorded of the detergent-solubilized purified QCR to monitor the influence of the mutations on the signal of the dithionite-reduced Rieske [2Fe-2S] cluster. Changes in shape and position of the signals can be interpreted as alterations of the ISP interaction with center P. As described previously, the EPR spectra of E272Q and wild-type QCR are nearly identical, whereas E272D differs in line shape and position compared with both of them, whereby the g_{zz} signal is markedly shifted to a higher magnetic field (12) (Table 3). Position and line shape of the EPR signal in F129R and Y132F QCR are also very similar compared with that of the wild-type enzyme. However, in all three variants of Tyr^{279}, the g_{zz} peak is again slightly shifted to higher magnetic fields. In addition, the g_{xx} peak of Y279S shows a pronounced shift (Fig. 3 and Table 3).

The signal of the reduced Rieske cluster of the F129K variant is less intense as compared with that of the wild type and cannot be clearly observed due to a strong spectral overlap with a signal of unknown origin with g values of 6.5, 5.3, and 2.0 (spectrum not shown). EPR signals with a similar line shape and resonance position compared with that of the latter have been reported for high spin ferric hemes, for instance in cytochrome *c* mutants, where the heme iron has lost one of its amino acid ligands (25). However, the signal observed here is dithionite-induced. Substitution of the aromatic residue by lysine may cause large structural rearrangements that affect not only inhibitor binding but the overall structure as well.

Pre-steady-state Reduction Kinetics of QCRs with Mutations in Cytochrome b at Tyr^{132} and Glu^{272}—To further investigate the role of conserved residues at center P on quinol oxidation, pre-steady-state reduction kinetics were measured of Tyr^{132} and Glu^{272} variants. We recently showed that Glu^{272} governs efficient ubiquinol oxidation preventing bypass reactions at center P (12). To further investigate its role in electron transfer, the pre-steady-state reduction kinetics of the E272D and E272Q variants were analyzed. The instability of the F129R/K variants precluded their analysis. We also did not measure the kinetics for variants of Tyr^{279}. These enzymes showed contaminations with several equivalents of cytochrome *c*, which overlaps spectroscopically with cytochrome c_1 and would have resulted in multiple turnovers of the enzyme, rendering pre-steady-state kinetics difficult to analyze. Furthermore, the pre-steady-state kinetics of the Y132F variant was measured. The phenylalanine substitution should disturb the suggested coupled proton/electron transfer (5, 6). Since the midpoint potentials of the heme groups are not shifted in the Y132F, E272D, and E272Q mutants, any alteration in electron transfer must result from other changes in these enzymes.

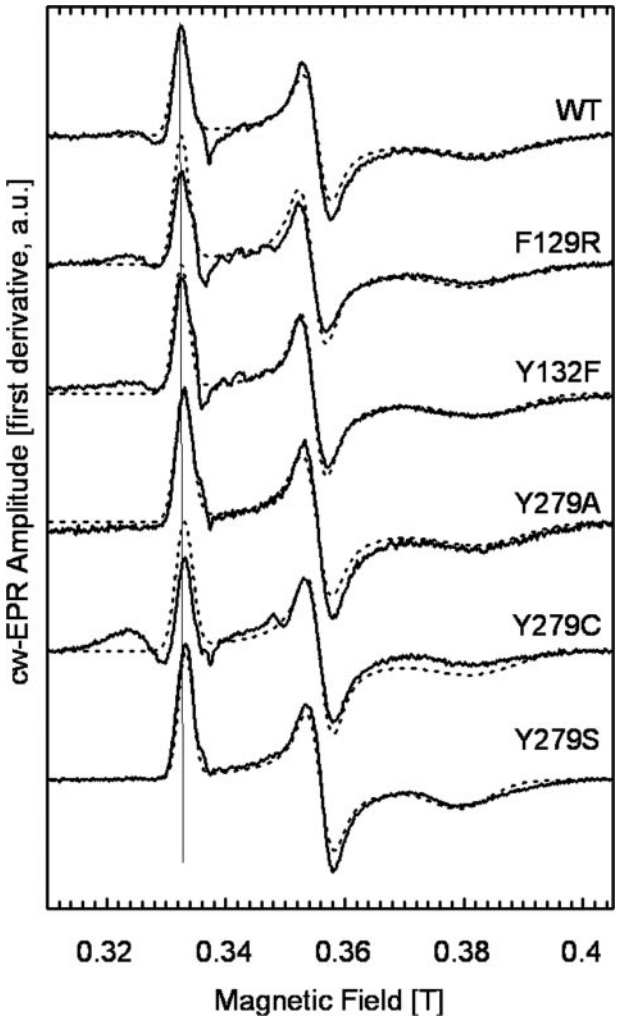

FIGURE 3. **Center P probed by electron paramagnetic resonance.** Continuous wave EPR spectra were recorded of detergent-solubilized and purified QCR reduced with an excess of dithionite (see "Experimental Procedures"). Values for g_{xx}, g_{yy}, and g_{zz} are presented in Table 3. Experimental conditions were as follows: microwave frequency, 9.42 GHz; microwave power, 1 milliwatt; modulation frequency, 100 kHz; modulation amplitude, 1.0 millitesla; temperature, 20 K.

TABLE 4

Ubiquinol-cytochrome *c* reductase activities of QCRs from wild-type yeast and from yeast with Y132F, E272Q, and E272D mutations in cytochrome *b*

Activities of the isolated enzymes were measured as described under "Experimental Procedures." TN, turnover number.

	TN	
	pH 7	pH 8.8
	s^{-1}	
Wild type	119	115
Y132F	41	34
E272D	37	32
E272Q	15	12

The selected enzymes were purified, and their respective turnover numbers at pH 7 and 8.8 were determined for comparison with the pre-steady-state measurements (Table 4). As expected, E272D and E272Q are slightly more active after single-step anion exchange chromatography compared with the two-step purification described previously (12). This increased catalytic activity can be attributed to less delipidation (22). The pre-steady-state measurements were carried out at pH 7 and 8.8. At pH 7, the E_m of the Rieske protein in wild-type QCR is ~15 mV higher than that of cytochrome c_1. As a result, the cytochrome c_1 will not be completely reduced during the first turnover, since the electron that is transferred into the high potential chain from the quinol will equilibrate to the Rieske protein (26). At pH 8.8, the E_m of the Rieske protein is about 70 mV lower than that of cytochrome c_1, resulting in ~80% reduction of the c_1 heme during the first pre-steady-state turnover of the enzyme. This is especially relevant when the enzyme is reduced in the presence of antimycin, which blocks any reduction through center N, which would indirectly affect the extent of c_1 reduction.

The pre-steady-state measurements were carried out with uninhibited enzyme and with inhibitors bound to center P or center N. By blocking center P with either stigmatellin or myxothiazol, reduction of cytochrome *b* via center N can be monitored. For those measurements, Y132F was inhibited with stigmatellin, since this variant is myxothiazol-resistant. The stigmatellin-resistant E272D and E272Q mutant enzymes were inhibited with myxothiazol. Alternatively, center N kinetics can also be monitored by cytochrome *b* reduction in the absence of any inhibitors, since the extents and rates of *b* reduction in this condition are very similar to those obtained in the presence of myxothiazol (center P blocked) but very different from those observed with antimycin (center N blocked). To investigate reduction of heme b_H and heme c_1 through center P, the enzymes were inhibited with antimycin.

In the uninhibited Y132F enzyme, the extent of heme c_1 reduction is diminished at both pH 7 and 8.8, and the rate of the first, faster phase of reduction at pH 7 is approximately half that of the wild-type enzyme. At pH 8.8, the amount of the first phase of reduction is so small (4%) that it cannot be accurately measured (Fig. 4). It should be noted that at pH 8.8 there is more reduction of the enzyme through center N than at pH 7, which obscures the effect of the change in E_m of the Rieske protein on the relative amounts of c_1 reduced at the two pH values. Partial reduction of cytochrome *b* through center N also results in inhibition of between 12% (pH 7) and 20% (pH 8.8) of center P sites even in the wild-type enzyme (Fig. 4). This missing c_1 absorbance is due to the lack of an acceptor for the second electron from ubiquinol oxidation in that fraction of the enzyme population where the b_H heme is already reduced.

For the E272Q enzyme, the extent of heme c_1 reduction is very similar to the wild-type enzyme, although the rate is significantly slower than that of the wild-type enzyme. For the E272D enzyme, the final extent of heme c_1 reduction is very similar to that of the wild-type enzyme at both pH values, but the rate of the fast phase is slower than that of the wild type at pH 7. At pH 8.8, the rate of the fast phase of c_1 reduction in the E272D mutant is similar to that of the wild type, although the percentage that undergoes rapid reduction is much less than the wild type (Fig. 5). However, the pH dependence of the cytochrome *c* reductase activity showed that the E272D enzyme had 28% of the wild-type turnover at pH 8.8 under steady-state conditions (Table 4). The Y132F mutant exhibits a marked decrease in extent of heme *b* reduction, which is also seen in the E272D enzyme, although to a lesser extent (Fig. 6). In addition,

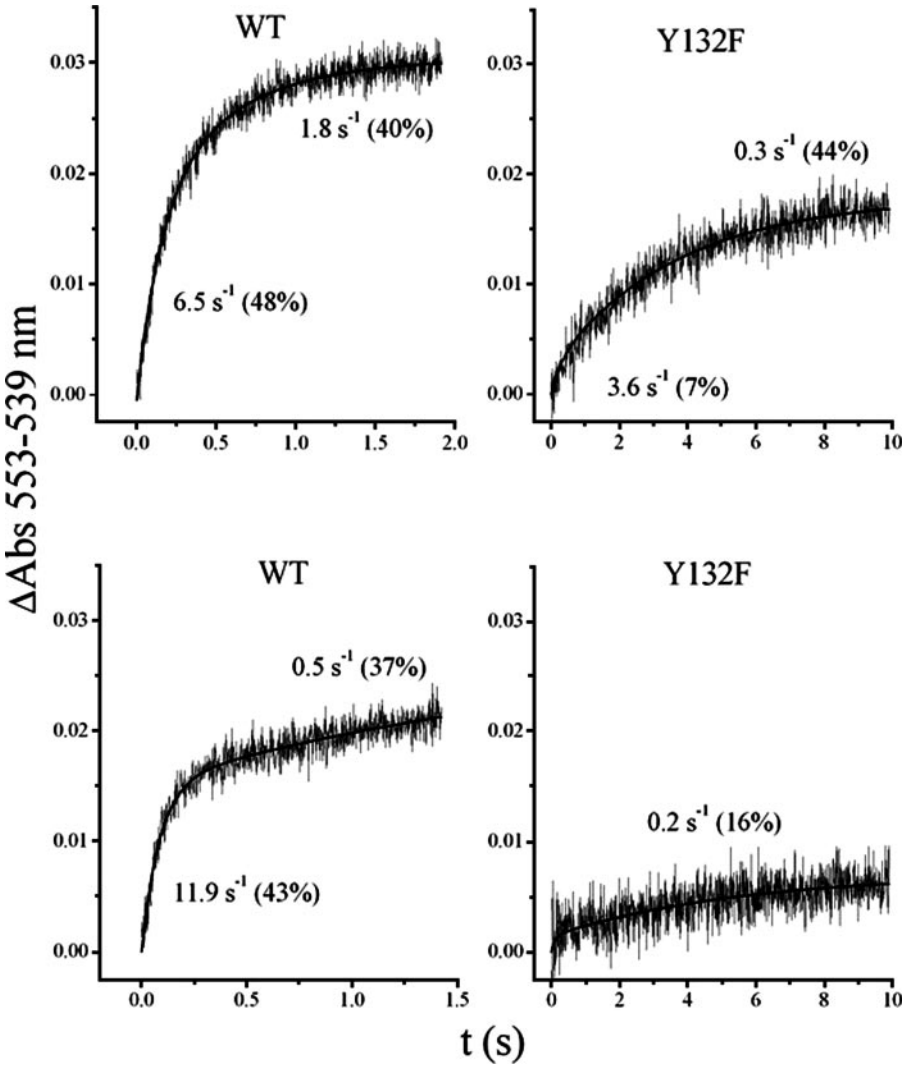

FIGURE 4. **Pre-steady-state reduction of cytochrome c_1 by ubiquinol in QCR from wild-type yeast and QCR with a Y132F mutation in cytochrome *b*.** The *top two panels* show reduction of the two enzymes by 20 μM DQH at pH 7.0, and the *bottom two panels* show reduction of the two enzymes at pH 8.8. Rates of c_1 reduction calculated from the *solid lines* are shown alongside the traces, and the percentage of reduction with the indicated rate is shown in *parentheses*. The absorbance obtained by reducing the enzyme with ascorbate (0.035) was used as the 100% reference value to calculate c_1 reduction percentages.

the Y132F and E272D enzymes show significant declines in the pre-steady-state rates, whereas the E272Q enzyme has faster rates than the wild type. We know that these rates reflect center N kinetics and not center P kinetics, because they are faster than the center P kinetics that are reflected in the fast phase of c_1 reduction at pH 8.8 (Figs. 3 and 4 *versus* Fig. 6).

The complete inhibition of heme b reduction by stigmatellin in the QCR from the Y132F mutant as shown in Fig. 7 is a further indication of a defect at center N in this enzyme. This suggests that the center P Y132F mutation causes a long range structural effect. It also appears that the presence of stigmatellin at center P has a slowing effect on the rate of b reduction through center N in the wild-type enzyme (Fig. 7 *versus* Fig. 6).

In the presence of antimycin at pH 8.8, center P in only one monomer is active during pre-steady-state reduction of the wild-type enzyme, and ~80% of the c_1 in that active monomer undergoes reduction after one turnover, as shown previously (14). Under these conditions, there is no interference from competing reduction of the *b* hemes through center N. We see essentially the same pattern of heme c_1 reduction as observed in Figs. 4 and 5 in the absence of inhibitors: decreased rate and extent of heme c_1 reduction in the Y132F mutant and decreased rate for most of the heme c_1 reduction in the E272Q and E272D enzymes (Fig. 8). The amount of heme c_1 reduction that appears to be rapid in the Y132F mutant is too small to reliably calculate a rate (Fig. 8).

The pronounced decline in the pre-steady-state rate of c_1 reduction in the Y132F enzyme seemed inconsistent with the catalytic activity of this enzyme (Table 1). We thus tested the effect of added cytochrome *c* on the pre-steady-state reduction of this enzyme. As shown in Fig. 9, the addition of one cytochrome *c* per dimer fully restores the extent of c_1 reduction that was lost in the Y132F mutant in the absence (Fig. 4) or presence (Fig. 8) of antimycin and increases by ~20 times the slow rate of heme c_1 reduction that was observed at pH 8.8. With the partial restoration of the heme c_1 reduction rate, the pre-steady-state rate is proportional to the catalytic rate when compared with the rates for the wild-type enzyme (Fig. 9 and Table 1).

DISCUSSION

In this work, we analyzed the effect of mutations at the ubiquinol oxidation site of the yeast mitochondrial QCR. We focused on mutations in the residues Phe^{129}, Tyr^{132}, Glu^{272}, and Tyr^{279} of cytochrome *b*. These residues with proposed functional implications are highly conserved in mitochondrial and bacterial QCRs (27, 28).

The residue Phe^{129} lines the hydrophobic substrate channel at center P, the side chain directed toward the hydrophobic cavity that facilitates substrate access to center P as well as to center N of the other monomer (Fig. 1). Phe^{129} is involved in binding of the hydrophobic tail of the inhibitor stigmatellin and presumably that of ubiquinol (5, 8). Substitution of the phenylalanine by lysine or arginine resulted in a lethal growth phenotype on nonfermentable carbon sources, clearly indicating a major limitation of QCR catalysis. Accordingly, the cytochrome *c* reductase activity of the F129K QCR was lowered to 27% of the wild-type rate. A similar decrease was observed for the bacterial mutant in the equivalent residue Phe^{144} (9, 29).

The purified QCR from the F129R mutant retained 84% of the wild-type turnover. It is surprising that this relative high

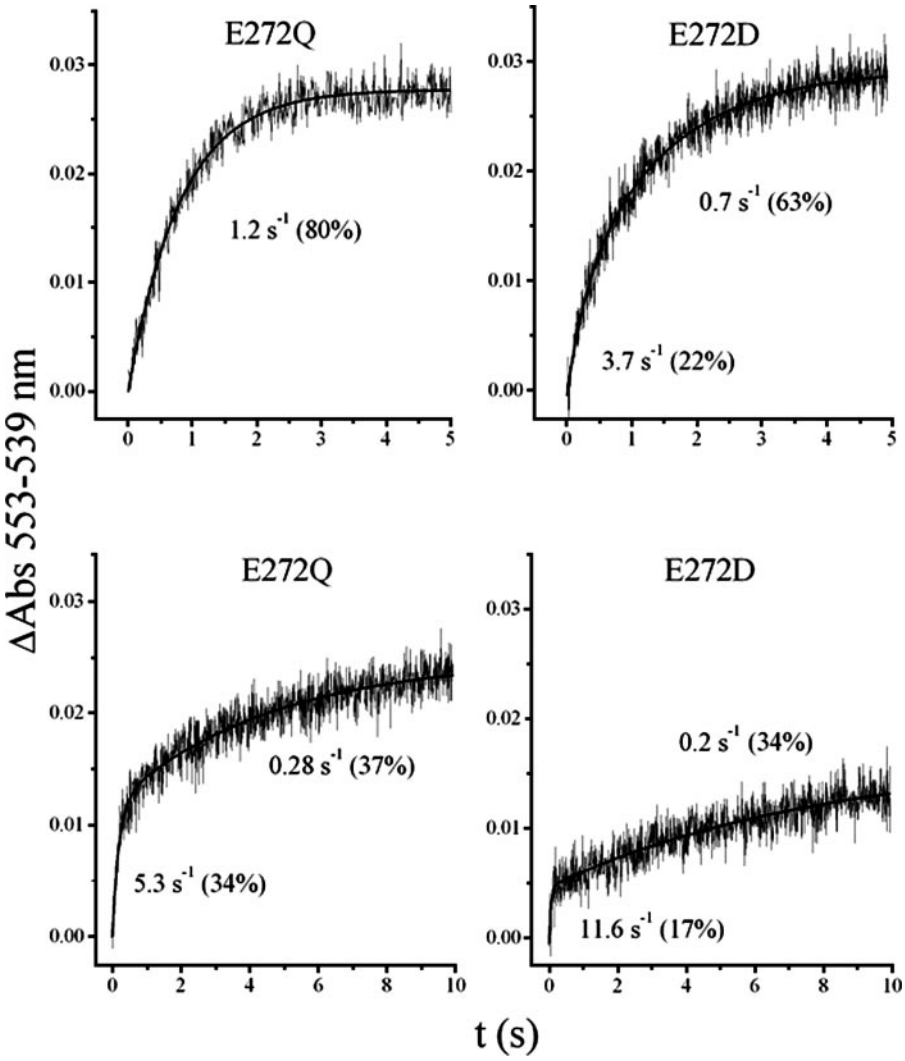

FIGURE 5. **Pre-steady-state reduction of cytochrome c_1 by ubiquinol in QCRs with E272D and E272Q mutations in cytochrome *b*.** The *top two panels* show reduction of the two enzymes by 20 μM DQH at pH 7.0, and the *bottom two panels* show reduction of the two enzymes at pH 8.8. Rates of c_1 reduction calculated from the *solid lines* are shown *beside* the *traces*, and the percentage of reduction with the indicated rate is in *parentheses*. The absorbance obtained by reducing the enzyme with ascorbate (0.035) was used as the 100% reference value to calculate c_1 reduction percentages.

catalytic rate does not sustain respiratory growth. The decreased QCR content in mitochondrial membranes obtained from cells grown in galactose medium suggests instability of this enzyme in the membrane. Accordingly, the F129R QCR had lower turnover numbers in the membrane, indicating that a part of the enzyme is inactive, which is then lost during purification. Furthermore, the variant enzyme was less stable during purification. The method had to be adapted by lowering the buffer flow to prevent disintegration of the multisubunit complex and concomitant loss of activity. Most likely, a higher lipid content improved stability and activity of the complex (6, 22).

The F129K QCR was insensitive to both stigmatellin and myxothiazol. Simultaneous resistance toward inhibitors of both center P domains was seen also in bacterial QCR, when the equivalent residue Phe^{144} was substituted by neutral residues as valine, glycine, leucine, and cysteine. This indicates that this residue forms a common surface of both inhibitor binding domains (9, 27, 30). Substitution of Phe^{129} by a charged residue will obviously abolish the observed nonpolar interaction with the hydrophobic tail of the inhibitor. This hinders not only binding of the inhibitors, as deduced from the resistance of F129K, but affects as well binding of the substrate, as indicated by the 5-fold increased K_m value for DQH (see Table 1). In agreement, replacement mutations with nonaromatic residues in the equivalent position Phe^{144} in bacterial QCR caused a major loss in affinity for the substrate, resulting in a partially depleted center P binding pocket (29). The F129R enzyme had decreased sensitivity for stigmatellin and myxothiazol as shown by increased IC_{50} values relative to the wild-type QCR. In contrast to the lysine substitution, the cytochrome *c* reductase activity could still be inhibited. Phe^{129} is part of a nonpolar patch at the cavity surface with the cytochrome *b* residues Leu^{130}, Phe^{179}, and Ile^{147} as direct neighbors. Introduction of lysine may lead to local structural changes. Arginine may be less disturbing, since its side chain is larger, and the guanidino group can form planar stacking interactions with aromatic residues and is more likely than lysine to participate in stabilizing cation-π interactions.

The midpoint potentials of both b hemes in the F129K variant were lowered by ~100 mV. These shifts will contribute to the slower catalytic turnover, since the driving force for electron transfer to the low potential chain is decreased. The shift may be caused by distortion of the heme coordination. An unexpected spectral overlap was observed for the [2Fe-2S] cluster EPR signal of the variant. In the equivalent bacterial mutation F144K, unusual [2Fe-2S] cluster spectral line shapes were described with shifted g_x and g_y values (29). Apparently, the replacement of the aromatic phenylalanine by the basic lysine causes structural perturbations at center P. A direct influence on heme b_L is conceivable, since Phe^{129} is located on a helix that parallels the cofactor, with the close residue Gly^{131} in van der Waals contact distance to the heme ligand His^{183} as well as to the protoporphyrin itself. The Phe^{129} side chain is not facing the heme but is pointing to the opposite side of the helix toward the center P cavity. The Glu^{272} side chain is $\leq$6 Å away from that of Phe^{129} without any other residue between. Substitution with the more flexible lysine may reorient the side chain, which could bring the amino group $\leq$4 Å and permit ion pair formation with Glu^{272}. The resulting

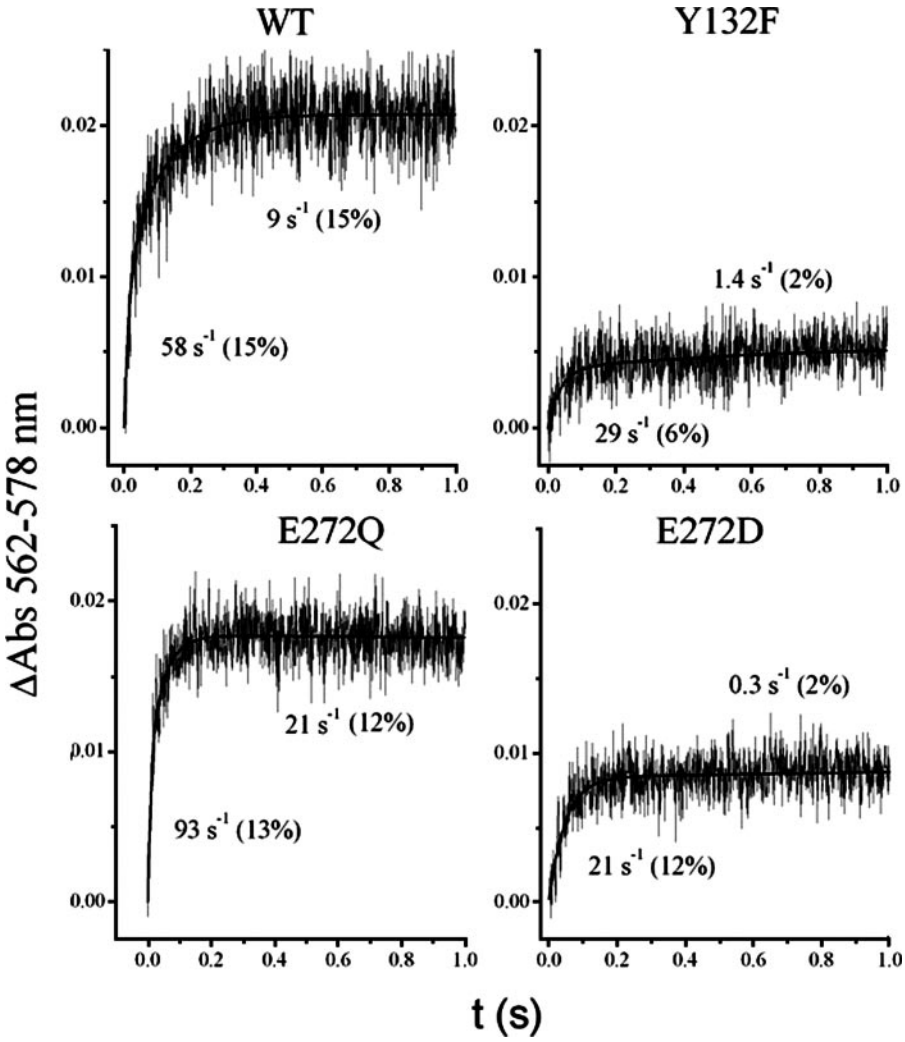

FIGURE 6. **Pre-steady-state reduction of cytochrome *b* by ubiquinol in QCRs from wild-type yeast and QCRs with a Y132F, E272Q, or E272D mutation in cytochrome *b*.** The traces show reduction of cytochrome *b* by 20 μM DQH at pH 7.0. Rates of *b* reduction calculated from the *solid lines* are shown *beside* the *traces*, and the percentage of b_H reduction with the indicated rate is in *parentheses*. The 100% value of b_H absorbance (0.072) was calculated by assuming that 70% of the total cytochrome *b* absorbance obtained in the dithionite minus ascorbate reduced spectrum (0.102) corresponded to the b_H heme.

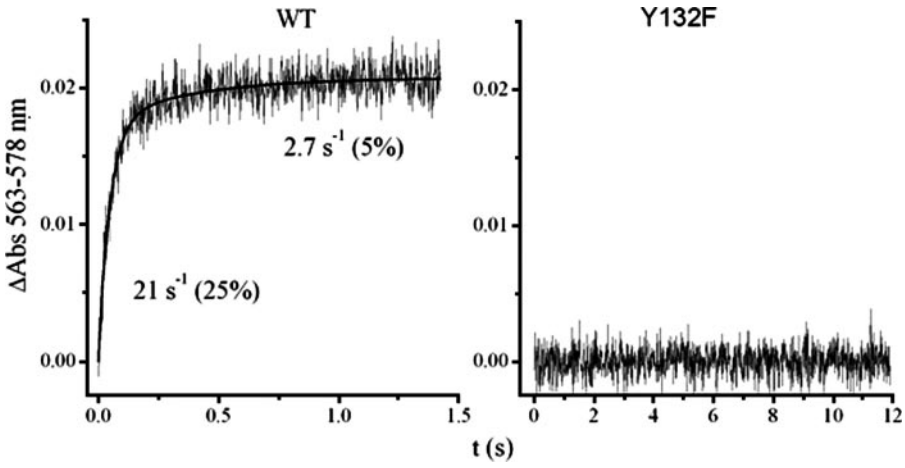

FIGURE 7. **Effect of stigmatellin on pre-steady-state reduction of cytochrome *b* by ubiquinol in QCR from wild-type yeast and QCR with a Y132F mutation in cytochrome *b*.** Enzymes were preincubated with 2 eq of stigmatellin prior to reduction with 20 μM DQH at pH 7. 0. Rates of b reduction calculated from the *solid lines* are shown *beside* the *trace* in the *left panel*, and the percentage of b_H reduction with the indicated rate is in *parentheses*. The 100% value of b_H absorbance (0.072) was calculated by assuming that 70% of the total cytochrome *b* absorbance obtained in the dithionite minus ascorbate reduced spectrum (0.102) corresponded to the b_H heme.

distortions could be sufficient to disturb the heme ligation and, in addition, would block Glu^{272} for substrate binding. In combination with the loss of a stabilizing interaction with the hydrophobic substrate tail, this would readily explain a lower affinity for the substrate ubiquinol indicated by an increased K_m value. Structural alterations are in line with a lowered H^+/e^- stoichiometry of the mutant enzyme, indicating an uncoupled Q cycle mechanism. Of all mutations analyzed in this and in a previous study (12), F129K is the only one with this marked effect on the ratio. Furthermore, this mutation results in a drastic increase in electron bypass reactions as judged by the superoxide production of the purified variant (~50% of total turnover), which is as high as in the E272Q enzyme (12).

The F129R mutation provoked less marked effects than the lysine substitution at this position. For F129R, the midpotential of heme b_L was only slightly increased by 20–30 mV, and the turnover was lowered to 84%. The EPR spectrum of the reduced F129R QCR is comparable with that of the wild-type enzyme, and the variant QCR exhibited an unchanged H^+/e^- stoichiometry. As discussed above, the arginine side chain with its capacity to interact with π-electron systems might be better suited to preserve the local architecture. However, the mutation affects the bifurcated electron transfer at center P, since superoxide production was increased to ~25% of the total cytochrome *c* reductase activity. This is nearly as high as for E272D, for which ~30% of the activity can be attributed to oxygen radical-producing bypass reactions (12).

Tyr^{279} has been postulated to participate in the positioning of the substrate ubiquinol (6). Alanine, serine, and cysteine replacements resulted in a distinct decrease of catalytic turnover (18, 25, and 55% of wild-type turnover, respectively). Apparently, the mutations make QCR a limiting step in respiratory

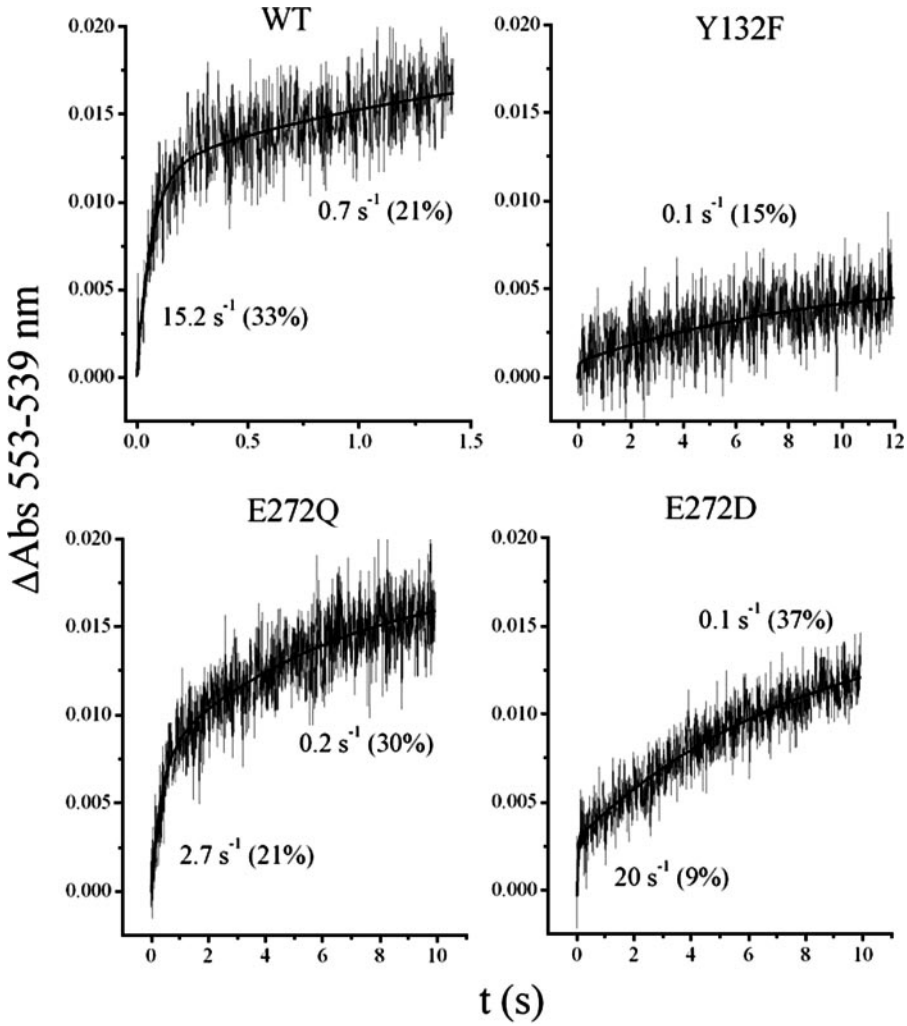

FIGURE 8. **Effect of antimycin on pre-steady-state reduction of cytochrome c_1 by ubiquinol in QCRs from wild-type yeast and QCRs with Y132F, E272Q, or E272D mutations in cytochrome *b*.** Enzymes were pre-incubated with 2 eq of antimycin prior to reduction with 20 μM DQH at pH 8. 8. Rates of c_1 reduction calculated from the *solid lines* are shown *beside* the *traces*, and the percentage of reduction with the indicated rate is in *parentheses*. The absorbance obtained by reducing the enzyme with ascorbate (0.035) was used as the 100% reference value to calculate c_1 reduction percentages.

growth, since the doubling times of the mutants increased ≥2-fold. Y279A and Y279C resulted in decreased sensitivity for the center P-specific inhibitors stigmatellin and myxothiazol, whereas Y279S even caused resistance to them. In a previous study, a shifted g_x signal in the EPR spectra of the Rieske protein was observed for mitochondrial membranes of Y279C and Y279A. It was interpreted as perturbed ubiquinol binding (13). EPR analysis of purified Y279A, Y279C, and Y279S QCRs (Table 3 and Fig. 3) showed an effect of these mutations on the environment of the [2Fe-2S] cluster, which was especially pronounced for the serine substitution. Our analysis of bypass reactions showed that superoxide production in the enzymes with Y279A, Y279C, and Y279S mutations was increased by 10–15%. The H^+/e^- ratio of the three variants was not affected. Taken together, the Tyr^{279} replacements with nonaromatic residues resulted in a 2–5-fold decrease in cytochrome *c* reductase activity combined with a low level of bypass reactions, suggesting that the mutations mainly alter the ubiquinol binding and consequently its oxidation but only to a smaller extent the bifurcated electron transfer.

To further investigate the role of center P residues in catalysis, we analyzed pre-steady-state reduction kinetics of the cytochromes in enzymes with mutations in Glu^{272} and Tyr^{132}. Both residues are located between the ubiquinol oxidation pocket and heme b_L. Glu^{272} was recently shown to govern efficient ubiquinol oxidation (12). The residue is highly but not fully conserved in cytochrome *b*, which might question its suggested role as proton acceptor for ubiquinol oxidation. We recently pointed out that in β- and γ-proteobacteria, in which this PEWY glutamate is replaced by valine or proline, at the position equivalent to His^{253} in yeast a glutamate is conserved. Based on structural considerations, we suggested that it can take over the proton transfer reaction (12). Tyr^{132} is one of the very few fully conserved cytochrome *b* residues (27, 29). Variants of these two residues exhibited decreased catalytic rates as compared with that of the wild-type enzyme (13% E272Q and 49% E272D (12); 48% Y132F (Table 1)) and increased superoxide production (~50% E272Q and ~30% E272D (12); ~20% Y132F). Furthermore, the K_m for DQH is increased by 8.4-fold for Y132F, the largest increase observed among the mutants described here as well as previously (12). The midpoint potentials of b and c_1 hemes were not affected in any of these mutants.

The Y132F enzyme exhibited disturbed electron transfer into the high potential chain as evident from diminished extent of cytochrome c_1 reduction upon ubiquinol addition at both pH 7.0 and 8.8. The disturbed reduction of the high potential chain is most evident at pH 8.8 (Fig. 4), where only 25% of the maximal reduction can be reached, whereas the cytochrome c_1 in the wild-type enzyme can be reduced to over 80%. A similar but less drastically disturbed reduction of cytochrome c_1 is observed for enzyme with the E272D mutation. In the E272D enzyme, the extent of cytochrome c_1 reduction was comparable with that in the wild-type enzyme, but the rate of reduction was decreased (Figs. 5 and 8). Very pronounced decreased reduction extent and disturbed kinetics were observed for the reduction of the b hemes in the presence of antimycin for both the Y132F and E272D variants. This result highlights a disturbed electron transfer to both high potential and low potential chains. In agreement, an increased superoxide production is observed for both of these mutations. It should be noted that the Y132F

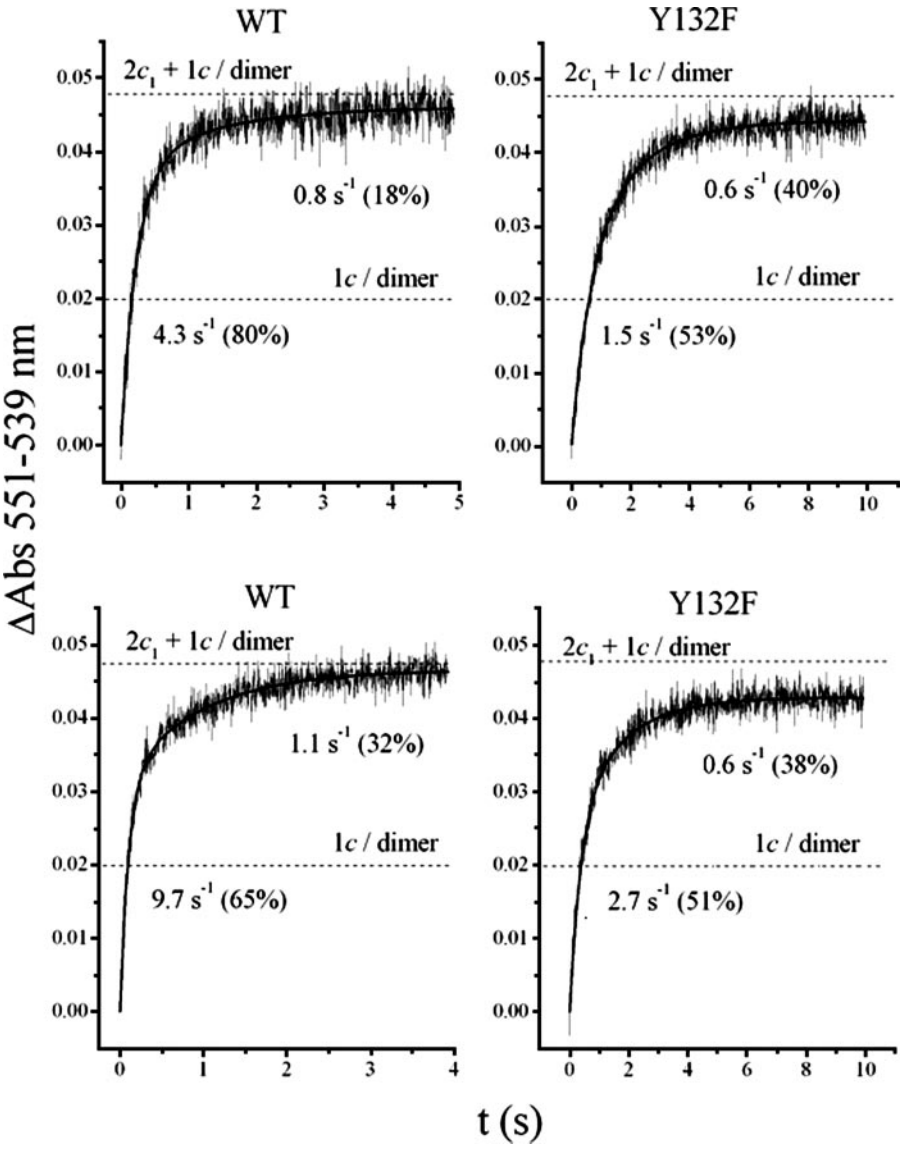

FIGURE 9. **Effect of cytochrome *c* on pre-steady-state reduction of cytochrome c_1 by ubiquinol in QCRs from wild-type yeast and QCRs with Y132F mutation in cytochrome *b*.** One equivalent of cytochrome *c* per QCR dimer was mixed with each complex prior to reduction of the enzymes with 20 μM DQH at pH 7.0 (*upper panels*) and pH 8.8 (*lower panels*). Rates of cytochrome $c + c_1$ reduction calculated from the *solid lines* are shown *beside* the *traces*, and the percentage of reduction with the indicated rate is in *parentheses*. The *horizontal dashed lines* indicate the expected absorbance changes resulting from complete reduction of 1 eq of cytochrome *c* or 1 eq of cytochrome *c* plus 2 eq of cytochrome c_1 per enzyme dimer. To calculate the expected absorbance changes at 551 nm for reduction of cytochrome *c* or reduction of cytochrome c_1 + cytochrome *c*, extinction coefficients of 20 mM^{-1} for cytochrome *c* and 13.7 mM^{-1} for cytochrome c_1 were used.

mutation, which has more pronounced effects on electron transfer at center P, shows less superoxide production than for the E272D substitution. Surprisingly, the pre-steady-state c_1 reduction extent of E272Q was not affected with respect to the wild-type enzyme, despite showing the lowest turnover numbers for cytochrome c reduction and the highest level of superoxide production. Yet, the rates were slowed down by a factor of 2–5. The observation that ubiquinol oxidation can still occur in the E272Q enzyme indicates that the second proton donated by ubiquinol oxidation is able to find a slower, less efficient pathway out of center P. Still, the significantly decreased center P rate highlights the relevance of Glu^{272} in the rate-limiting step of ubiquinol oxidation.

To analyze the influence of the center P mutations on center N kinetics, ubiquinol oxidation through center P was blocked with inhibitors. Electron transfer at center N was completely inhibited by the Y132F mutation when electron transfer through center P was inhibited with stigmatellin. The Y132F mutation also caused a decrease in the extent of reduction of the b hemes via center N. Thus, the mutation at center P apparently prevents electron transfer at the quinone reduction site, indicating long range interactions within the protein. The same result was seen for the enzyme with the E272D mutation. Since no changes in the heme midpoint potentials of the Y132F and E272D enzymes were observed, the disturbed electron transfer either indicates that the substituted residues are not functionally equivalent or that the structure is perturbed. Our previous study indicates an altered environment of the Rieske protein in the E272D enzyme, as evident from shifted signals in the EPR spectrum of the reduced [2Fe-2S] cluster (12). This result indicates a modified binding mode of the ubiquinol, which might influence its oxidation and the electron transfer.

In addition, the observed effects on pre-steady-state kinetics might be related to malfunction of the proposed parallel proton/electron transfer route from center P to heme b_L that involves rotational displacement of Glu^{272} (5, 6). The shorter aspartate side chain could disrupt the proton relay. Similarly, the loss of the hydroxyl group by the Y132F mutation will destabilize the position of a water molecule, which is part of the suggested pathway and thereby affect coupled electron/proton transfer.

Interestingly, the addition of one molecule cytochrome *c* per QCR dimer accelerated the reduction of the c_1 heme in both the Y132F and E272D enzymes so that the pre-steady-state rates were consistent with the rates observed in the steady-state experiments. Apparently, cytochrome *c* binding activates the complex and enhances electron transfer, suggesting that structural alterations occur at center P in the mutated enzymes upon binding of the cytochrome *c*.

In conclusion, in the present study, we could show that lysine substitution of Phe^{129}, which is exposed in the hydrophobic substrate channel, leads to a negative respiratory growth phe-

notype with increased bypass reactions, uncoupling of the Q cycle, disturbed substrate binding, and shifted b heme midpoint potentials. The F129R mutant is less severely affected, suggesting that the structural integrity is better preserved. We could also show that substitutions of Tyr^{279}, where mutations cause human mitochondrial disease, affect quinol binding and oxidation with little influence on electron transfer bypass reactions.

Mutations in Glu^{272} and Tyr^{132} markedly affect center P catalysis, lowering the catalytic activity and elevating bypass reactions. Interestingly, mutations at center P that disturb ubiquinol oxidation, such as the Y132F and E272D, also strongly influence electron transfer kinetics at center N. This suggests a long range structural interaction between center P and center N. Another novel finding was that cytochrome *c* binding restores electron transfer in center P mutants that showed disturbed reduction of both high potential and low potential chains. This suggests that cytochrome *c* binding can elicit structural changes at center P. Crystallographic studies of yeast QCR with cytochrome *c* bound previously suggested a correlation of cytochrome *c* binding with center N quinone occupancy (23).

The detailed characterization of the mutations supports the importance of all targeted residues for correct center P catalysis and discriminates the individual properties of the residues with respect to substrate binding and oxidation, bifurcated electron transfer, bypass reactions, and structural integrity. X-ray structure analysis of selected variants is in progress. The catalysis of ubiquinol oxidation is a robust process. Residual enzyme activity is observed in all cases, even with severe effects that abolish respiratory growth or disrupt heme ligation. However, all analyzed mutations provoke superoxide production, indicating that these residues are required for efficient catalysis to prevent bypass reactions deleterious for the organism.

Acknowledgments—We thank Philipp Harbach and Lukas Hubener for practical assistance with the EPR studies.

REFERENCES

1. Mitchell, P. (1976) *J. Theor. Biol.* **62,** 327–367
2. Hunte, C., Palsdottir, H., and Trumpower, B. L. (2003) *FEBS Lettr.* **545,** 39–46
3. Osyczka, A., Moser, C. C., and Dutton, P. L. (2005) *Trends Biochem. Sci.* **30,** 176–182
4. Crofts, A. R. (2004) *Annu. Rev. Physiol.* **66,** 689–733
5. Hunte, C., Koepke, J., Lange, C., Rossmanith, T., and Michel, H. (2000) *Structure* **8,** 669–684
6. Palsdottir, H., Lojero, C. G., Trumpower, B. L., and Hunte, C. (2003) *J. Biol. Chem.* **278,** 31303–31311
7. Kim, H., Xia, D., Yu, C. A., Xia, J. Z., Kachurin, A. M., Zhang, L., Yu, L., and Deisenhofer, J. (1998) *Proc. Natl. Acad. Sci. U. S. A.* **95,** 8026–8033
8. Esser, L., Quinn, B., Li, Y. F., Zhang, M., Elberry, M., Yu, L., Yu, C.-A., and Xia, D. (2004) *J. Mol. Biol.* **341,** 281–302
9. Brasseur, G., Saribas, A. S., and Daldal, F. (1996) *Biochim. Biophys. Acta* **1275,** 61–69
10. Crofts, A. R., Hong, S., Ugulava, N., Barquera, B., Gennis, R., Guerova-Kuras, M., and Berry, E. (1999) *Proc. Natl. Acad. Sci. U. S. A.* **96,** 10021–10026
11. Crofts, A. R., Barquera, B., Gennis, R. B., Kuras, R., Guerova-Kuras, M., and Berry, E. A. (1999) *Biochemistry* **38,** 15807–15826
12. Wenz, T., Hellwig, P., MacMillan, F., Meunier, B., and Hunte, C. (2006) *Biochemistry* **45,** 9042–9052
13. Fisher, N., Castleden, C. K., Bourges, I., Brasseur, G., Dujardin, G., and Meunier, B. J. (2004) *J. Biol. Chem.* **279,** 12951–12958
14. Covian, R., and Trumpower, B. L. (2005) *J. Biol. Chem.* **280,** 22732–22740
15. von Jagow, G., and Link, T. A. (1986) *Methods Enzymol.* **126,** 253–271
16. Sarbias, A. S., Ding, H., Dutton, P. L., and Daldal, F. (1992) *Biochemistry* **34,** 16004–16012
17. Geier, B. M., Schagger, H., Brandt, U., Colson, A. M., and von Jagow, G. (1992) *Eur. J. Biochem.* **208,** 375–380
18. Jordan, D. B., Livingston, R. S., Bisaha, J. J., Duncan, K. E., Pember, S. O., Picollelli, M. A., Schwartz, R. S., Sternberg, J. A., and Xiao-Song, T. (1999) *Pestic. Sci.* **55,** 105–188
19. Fisher, N., and Meunier, B. (2005) *Pest. Manag. Sci.* **61,** 973–978
20. Wibrand, F., Ravn, K., Schwartz, M., Rosenberg, T., Horn, N., and Vissing, J. (2001) *Ann. Neurol.* **50,** 540–543
21. Kessl, J. J., Hill, P., Lange, B. B., Meshnick, S. R., Meunier, B., and Trumpower, B. L. (2004) *J. Biol. Chem.* **279,** 2817–2824
22. Palsdottir, H., and Hunte, C. (2004) *Biochim. Biophys. Acta* **1666,** 2–18
23. Lange, C., and Hunte, C. (2002) *Proc. Natl. Acad. Sci. U. S. A.* **99,** 2800–2805
24. Muller, F., Crofts, A. R., and Kramer, D. M. (2002) *Biochemistry* **41,** 7866–7874
25. Silkstone, G. G., Copper, C. E., Svistunenko, D., and Wilson, M. T. (2005) *J. Am. Chem. Soc.* **127,** 92–99
26. Covian, R., Gutierrez-Cirlos, E. B., and Trumpower, B. L. (2004) *J. Biol. Chem.* **279,** 15040–15049
27. Degli Esposti, M., de Vries, S., Crimi, M., Ghelli, A., Patarnello, T., and Meyer, A. (1993) *Biochim. Biophys. Acta* **1143,** 243–271
28. Nitschke, W., Lebrun, E, Santini, J., Brugna, M. E., Ducluzeau, A.-L., Ouchane, S., Schoepp-Cothenet, B., and Baymann, F. (2006) *Mol. Biol. Evol.* **23,** 1180–1191
29. Ding, H., Moser, C. C., Robertson, D. E., Tokito, M. K., Daldal, F., and Dutton, P. L. (1995) *Biochemistry* **34,** 15979–15996
30. Di Rago, J. P., Copee, J. Y., and Colson, A. M. (1989) *J. Biol. Chem.* **264,** 14543–14548